

# Molecular Dynamics Simulation of Water Mobility in Magnesium-Smectite Hydrates

Jeffery A. Greathouse,<sup>\*,†,‡</sup> Keith Refson,<sup>§</sup> and Garrison Sposito<sup>‡</sup>

Contribution from the Department of Chemistry, St. Lawrence University, Canton, New York 13617, Department of Earth Sciences, Oxford University, Parks Road, Oxford OX1 3PR, UK, and Geochemistry Department, Earth Sciences Division, Mail Stop 90/1116, Lawrence Berkeley National Laboratory, Berkeley, California 94720

Received May 30, 2000. Revised Manuscript Received August 14, 2000

**Abstract:** Water diffusion and interlayer structure in Mg-smectite hydrates was investigated by molecular dynamics and Monte Carlo computer simulation. Smectites with only tetrahedral layer charge (Mg-beidellite) were examined at 300 and 400 K, each with two layers of adsorbed water. Previous quasielastic neutron-scattering experiments have indicated that nonsolvating water molecules in Mg-smectites exhibit faster diffusional motion within a “cage” formed by the solvated  $\text{Mg}(\text{H}_2\text{O})_6^{2+}$  counterions than they do via inter-cage motion. Our 500–1175 ps MD simulations suggested that the dimension of this “cage” region is approximately 5.5 Å, but two-phase diffusional behavior was observed only for water in Mg-beidellite at 300 K. The counterions in Mg-beidellite formed outer-sphere surface complexes with the clay mineral siloxane surface, but nonsolvating water molecules showed a significant tendency to occupy ditrigonal cavities in the surface. This behavior could be responsible for the small equilibrium layer spacing in Mg-beidellite, as well as a lower water self-diffusion coefficient.

## 1. Introduction

The dominant role played by bivalent metal counterions in the organization of water molecules in the interlayer of hydrated smectite clay minerals has long been appreciated.<sup>1,2</sup> For these clay minerals, which are isostructural to mica but have smaller layer charge created by isomorphous cation substitutions,<sup>1</sup> the mere presence of bivalent metal counterions ( $\text{Sr}^{2+}$ ,  $\text{Ca}^{2+}$ ,  $\text{Mg}^{2+}$ ) with their strong solvation characteristics is sufficient to determine the extent of water vapor adsorption under given conditions and the degree of hydrogen bonding in the resultant interlayer network of adsorbed molecules.<sup>3–7</sup> Much less is known, however, about the mobility of water molecules in the interlayers of these smectite hydrates. The few available data<sup>2,8</sup> suggest that the residence times of nonsolvating water molecules are only about 1 order of magnitude longer than those in bulk water (5 ps at 298 K<sup>1</sup>). The solvation-shell water molecules are

similar in mobility to solvation-shell water molecules in ionic solutions of bivalent metal cations,<sup>1,9</sup> whereas the nonsolvating water molecules are more similar in behavior to those in the bulk liquid, but evidently are slowed considerably by their interactions with the clay mineral surface and the constrained geometry of the interlayer.

Molecular simulation can provide useful insight into the behavior of aqueous systems—particularly when there is a paucity of available data—as part of the development of improved experimentation. Recent Monte Carlo and molecular dynamics studies of hydrated smectites with monovalent counterions<sup>9–12</sup> have proved valuable in this way, but comparable investigations of these systems with bivalent counterions are lacking. Skipper et al.<sup>13,14</sup> have investigated the one- and two-layer hydrates of Otay-type<sup>1</sup> Mg-montmorillonite using Monte Carlo simulation. Their calculations revealed an equilibrium distribution of counterions on the interlayer midplane, with each  $\text{Mg}^{2+}$  surrounded by an octahedral solvation shell. Extensive hydrogen bonding between nonsolvating water molecules and the siloxane surface<sup>1</sup> of the clay mineral also was observed, as were water molecules attracted into the ditrigonal cavities<sup>1</sup> of the surface. Overall,  $\text{Mg}^{2+}$ –water interactions strongly influenced the interlayer water configuration. Refson

\* Address correspondence to this author at the following e-mail address: jgreathouse@stlawu.edu.

† St. Lawrence University.

‡ Oxford University.

§ Lawrence Berkeley National Laboratory.

(1) Sposito, G. *The Surface Chemistry of Soils*; Oxford University Press: New York, 1984; Chapters 1 and 2. This reference may be consulted for clay mineral terminology.

(2) Güven, N. In *Clay–Water Interface and its Rheological Implications*; Güven, N., Pollastro, R. M., Eds.; The Clay Minerals Society: Boulder, CO, 1992; Chapter 1.

(3) Prost, R. *Ann. Agron.* **1975**, *26*, 463–535.

(4) Brindley, G. W.; Brown, G. *Crystal Structures of Clay Minerals and their X-ray Identification*; Mineralogical Society: London, 1980; Chapter 3.

(5) Brown, D. R.; Kevan, L. *J. Am. Chem. Soc.* **1988**, *110*, 2743–2748.

(6) Johnston, C. T.; Sposito, G.; Erickson, C. *Clays Clay Miner.* **1992**, *40*, 722–730.

(7) Cases, J. M.; Bérend, I.; François, M.; Uriot, J. P.; Michot, L. J.; Thomas, F. *Clays Clay Miner.* **1997**, *45*, 8–22.

(8) Tuck, J. J.; Hall, P. L.; Hayes, M. H. B.; Ross, D. K.; Hayter, J. B. *J. Chem. Soc., Faraday Trans. 1* **1985**, *81*, 833–846.

(9) Ohtaki, H.; Radnai, T. *Chem. Rev.* **1992**, *92*, 1157–1204.

(10) Boek, E. S.; Coveney, P. V.; Skipper, N. T. *J. Am. Chem. Soc.* **1995**, *117*, 12608–12617.

(11) Boek, E. S.; Coveney, P. V.; Skipper, N. T. *Langmuir* **1995**, *11*, 4629–4631.

(12) Chang, F.-R. C.; Skipper, N. T.; Refson, K.; Greathouse, J. A.; Sposito, G. In *Mineral–Water Interface Reactions*; Sparks, D. L., Grundl, T., Eds.; American Chemical Society: Washington, DC, 1998; Chapter 6.

(13) Skipper, N. T.; Refson, K.; McConnell, J. D. C. *J. Chem. Phys.* **1991**, *94*, 7434.

(14) Skipper, N. T.; Refson, K.; McConnell, J. D. C. In *Geochemistry of Clay–Pore Fluid Interactions*; Manning, D. C., Hall, P. L., Hughs, C. R., Eds.; Chapman and Hall: London, 1993; Chapter 2.

et al.,<sup>15</sup> using molecular dynamics simulation, studied the mobility of  $\text{Mg}^{2+}$  and of water molecules in the interlayer region of the system investigated by Skipper et al.<sup>13,14</sup> Over the 15–40 ps simulation time, solvation-shell water molecules did not exit their positions, but the nonsolvating water molecules moved about the interlayer region readily, unless they were hindered by attraction into a ditrigonal cavity. Estimated self-diffusion coefficients for these water molecules were in qualitative agreement with experiment,<sup>8</sup> after scaling them to take into account the nonmobile fraction of interlayer water solvating the counterions.

In addition to providing information regarding the structure and dynamics of chemical systems, molecular simulation serves as a method to assess the various models used in fitting experimental data. For example, the methods used in analyzing neutron scattering experiments of water adsorbed onto clay minerals involve a degree of approximation.<sup>16</sup> Tuck et al.<sup>8</sup> performed quasielastic neutron scattering experiments on aqueous Ca- and Mg-substituted vermiculite, a clay mineral which bears negative charge only in the tetrahedral layer, to determine the water self-diffusion coefficient in each case. Because they observed different values for the self-diffusion coefficient on the two time scales of the instruments used, the authors concluded that water molecules in this hindered environment undergo a faster motion on short time scales and a slower motion on long time scales.<sup>8</sup> As a means to further investigate these experimental results, we report improved molecular dynamics (MD) and Monte Carlo (MC) simulations of interlayer mobility and water structure in the two-layer hydrate of Mg-smectite. Our MD simulations, ranging over 500 to 1175 ps, greatly exceed the time scales probed in the pioneering study of Refson et al.<sup>15</sup> Because our MD simulations were performed under the constraint of constant pressure rather than the more common constraint of constant volume,<sup>15,17</sup> the  $d(001)$  spacing<sup>1</sup> is a dynamical quantity. The model smectite we investigated was beidellite, a dioctahedral clay mineral which has layer charge originating only in its tetrahedral sheet.<sup>1</sup> The principal objectives of our study thus were to assess the effects of tetrahedral layer charge on interlayer water mobility in Mg-smectites, as well as to examine this mobility more completely, over time scales that are accessible to a variety of spectroscopic methods<sup>1,2</sup> which have been used to investigate molecular behavior in clay mineral hydrates.

## 2. Simulation Methods

**2.1. Model Clay Minerals and Potential Functions.** The clay mineral was selected so as to examine the effect of tetrahedral layer charge on the behavior of interlayer  $\text{Mg}^{2+}$ . Beidellite is a 2:1 layer type aluminosilicate in the smectite group:<sup>1</sup>



where [ ] indicates cations in the tetrahedral sheet and ( ) indicates cations in the octahedral sheet. Beidellite is a dioctahedral smectite with isomorphic substitution of  $\text{Al}^{3+}$  for  $\text{Si}^{4+}$  in its tetrahedral sheets.<sup>1</sup> In the unit-cell formula given above, these substitutions lead to a layer charge (moles of excess negative charge per mole of unit cells<sup>1</sup>) of 0.75e which is balanced by interlayer  $\text{Mg}^{2+}$  counterions, shown immediately to the left of the tetrahedral-sheet cations in the unit-cell formula. We employ a rigid framework for the clay lattice that has

(15) Refson, K.; Skipper, N. T.; McConnell, J. D. C. In *Geochemistry of Clay-Pore Fluid Interactions*; Manning, D. C., Hall, P. L., Hugs, C. R., Eds.; Chapman and Hall: London, 1993; Chapter 3.

(16) Sposito, G.; Prost, R. *Chem. Rev.* **1982**, *82*, 553–573.

(17) Greathouse, J. A.; Sposito, G. *J. Phys. Chem. B* **1998**, *102*, 2406–2414.

**Table 1.** Effective-Charge Parameters for Beidellite<sup>18</sup>

atom	$q(e)$	description
O ( $T_d$ apical)	-1.0, -1.19 <sup>a</sup>	apical oxygen atom in tetrahedral layer
O (surface)	-0.8, -0.99 <sup>a</sup>	surface oxygen in tetrahedral layer
O(H) (clay)	-1.7175	hydroxyl oxygen in octahedral layer
(O)H (clay)	0.7175	hydroxyl hydrogen in octahedral layer
Si ( $T_d$ )	1.2	silicon in tetrahedral layer
Al ( $T_d$ )	0.2, 0.96 <sup>a</sup>	aluminum in tetrahedral layer
Al ( $O_h$ )	3.0	aluminum in octahedral layer
Mg(int)	2.0	interlayer magnesium ion

<sup>a</sup> Second value used in molecular dynamics simulations.

been used successfully to predict  $d(001)$  layer spacings, interlayer structure, and water self-diffusion coefficients.<sup>10–21</sup> Teppen et al.<sup>22</sup> have used a flexible model for clay minerals that allows for full movement of the M–O–M bonds in the clay structure, where M represents Si, Al, or other cations in the octahedral sheet. A flexible atom model allows for structural relaxation and produces lower equilibrium energies than a rigid atom model. However, our rigid atom model is computationally more efficient, allowing for simulations in the nanosecond regime.

Our simulation techniques are based on classical Monte Carlo and molecular dynamics methods, which are well suited to investigate the equilibrium structure and long-time dynamics of complex systems. Water molecules are treated as rigid bodies, thus interatomic interactions are in the form of long-range Coulomb interactions and short-range van der Waals interactions. Effective-charge parameters ( $q$ ) for ions in the model clay mineral are listed in Table 1. Full discussion of the semiempirical computations on atomic clusters that were used in making the estimates of the  $q$ -values is given by Skipper et al.<sup>13,18</sup> The sensitivity of the simulated structure to the effective charge parameters used for Al( $T_d$ ) was investigated by performing MD runs using two different values for Al( $T_d$ ). These were 0.2e and 0.96e, and the neighboring O charges were adjusted to maintain charge-balance. There was no measurable difference between the equilibrium layer spacings or the water self-diffusion coefficient computed with the two values of Al( $T_d$ ). However, water molecules were slightly more likely to adsorb into ditrigonal cavities on the clay surface with the lower Al charge.

Our short-range interatomic potential parameters are based on the water model of Matsuoka, Clementi, and Yoshimine (MCY), which was developed from ab initio calculations of the water dimer.<sup>23</sup> The model potential function used to represent the interactions smectite–smectite, smectite–water, counterion–counterion, counterion–water, and water–water is given by the MCY form:<sup>13,18,19</sup>

$$U(r_{ij}) = \sum_{i=1}^N \sum_{j \neq i}^N \left[ \frac{q_i q_j}{r_{ij}} - A_{ij} e^{-B_{ij} r_{ij}} + C_{ij} e^{-D_{ij} r_{ij}} \right] \quad (1)$$

The van der Waals parameters ( $A$ ,  $B$ ,  $C$ ,  $D$ ) describing short-range interactions between atoms in the water–counterion–clay systems are the same as were used by Skipper et al.<sup>13</sup> and by Greathouse and Sposito,<sup>17</sup> except for the Mg(int)–Al( $T_d$ ) and Mg(int)–Si( $T_d$ ) interactions, for which  $A = B = 0$ ,  $C = 619.804 \text{ kcal mol}^{-1}$ , and  $D = 1.1839 \text{ \AA}$ . Short-range interactions in eq 1 were subjected to a 9 Å real-space cutoff. The values of the effective-charges and the van der Waals parameters for interaction between water molecules were taken from the MCY model,<sup>23,24</sup> as discussed by Skipper et al.,<sup>13,18</sup> who provide

(18) Skipper, N. T.; Chang, F.-R. C.; Sposito, G. *Clays Clay Miner.* **1995**, *43*, 285–293.

(19) Skipper, N. T.; Refson, K.; McConnell, J. D. C. *Clay Miner.* **1989**, *24*, 411.

(20) Park, S.-H.; Sposito, G. *J. Phys. Chem. B* **2000**, *104*, 4642–4648.

(21) Chang, F.-R. C.; Skipper, N. T.; Sposito, G. *Langmuir* **1995**, *11*, 2734–2741.

(22) Teppen, B. J.; Rasmussen, K.; Bertsch, P. M.; Miller, D. M.; Schäfer, L. *J. Phys. Chem. B* **1997**, *101*, 1579–1587.

(23) Matsuoka, O.; Clementi, E.; Yoshimine, M. *J. Chem. Phys.* **1976**, *64*, 1351–1361.

(24) Beveridge, D. L.; Mezei, M.; Mehrotra, P. K.; Marchese, F. T.; Ravi-Shanker, G.; Vasu, T.; Swaminathan, S. In *Molecular-Based Study of Fluids*; Haile, J. M., Mansorrit, G. A., Eds.; American Chemical Society: Washington, DC, 1983; pp 297–351.

evidence for their reliability in the simulation of interlayer water structure. Sposito et al.<sup>25</sup> have shown recently that the MCY model, when constrained to the equilibrium density of bulk liquid water, accurately predicts its radial distribution functions for O–O, O–H, and H–H spatial correlations as determined by the latest available isotopic-difference neutron diffraction data on D<sub>2</sub>O/H<sub>2</sub>O mixtures. Park and Sposito<sup>20</sup> have found the same for MCY-based predictions of the total radial distribution function of interlayer water in Li- and Na-montmorillonite hydrates. The MCY potential function also compares very well with the more recently developed anisotropic site potential functions<sup>26</sup> in calculations of the second virial coefficient of water vapor over a broad temperature range, as well as in predicting the geometry and binding energy of the water dimer.<sup>27</sup> Both of these potential functions were superior in this respect to the TIP4P potential function.<sup>28</sup> Chang et al.<sup>29</sup> also have demonstrated the comparative reliability of the MCY potential function over TIP4P in their simulations of interlayer water structure in Li-montmorillonite hydrates.

**2.2. Simulations.** The simulation cell used is a 21.12 Å × 18.28 Å patch with two half-layers of the clay mineral extending over eight unit cells.<sup>13,18</sup> Structural OH groups form an angle of 23° with the basal plane, in accordance with structural data for dioctahedral smectites.<sup>4</sup> Negative charge sites in beidellite reside in the tetrahedral layer only,<sup>4</sup> and these sites are created by replacing six Si atoms with Al atoms in as disordered a structure as allowed by the periodic boundary conditions. The Al charge is then reduced from +1.2e to +0.96e, and the charges on neighboring O atoms are adjusted to achieve a net charge of –6.0e. This substitution scheme was used previously in simulations of Li-beidellite<sup>17</sup> with three charge sites each in the upper and lower clay layers, respectively. The clay layer structure is unchanged by these substitutions, and although we have not performed quantum chemical calculations to investigate the degree of lattice disorder caused by tetrahedral substitution, our beidellite and montmorillonite models have compared well with available experimental data.<sup>10–21</sup> The simulation cell was replicated infinitely in three dimensions to mimic a physically observable macroscopic system. Short-range interactions were treated with the all-image convention, and long-range Coulombic interactions across (or beyond) the simulation cell were computed by the Ewald sum method<sup>30</sup> with a 2 Å<sup>-1</sup> reciprocal-space cutoff. The interlayer region of the simulation cell contained three Mg<sup>2+</sup> counterions and 64 water molecules, corresponding to a two-layer hydrate.

Monte Carlo simulations were performed on a Cray J90 supercomputer using the code MONTE<sup>31</sup> in a constant (NσT) ensemble, where absolute temperature (*T*) and the pressure applied normal to the clay layers (*σ*) are kept constant at 300 K and 100 kPa, respectively. The phase-space sampling strategy we followed has been described in detail previously.<sup>12,29</sup> Briefly, with the initial clay layer spacing set at 16.0 Å, water molecules were placed randomly within the interlayer, and Mg<sup>2+</sup> counterions were placed randomly on the midplane between clay layers. Only water molecules were allowed to move for the first 100 000 steps, followed by 2 400 000 steps in which movement of all interlayer species was allowed. A MC move could involve a water molecule, an interlayer Mg<sup>2+</sup>, or the upper clay layer. Layer–layer Coulombic interactions were not included in potential energy calculations. Convergence profiles for the total potential energy and the layer spacing were monitored to determine equilibration.<sup>18</sup>

The code MOLDY,<sup>32</sup> run on a Silicon Graphics Origin 2000 supercomputer, was used for MD simulations. A nonequilibrated

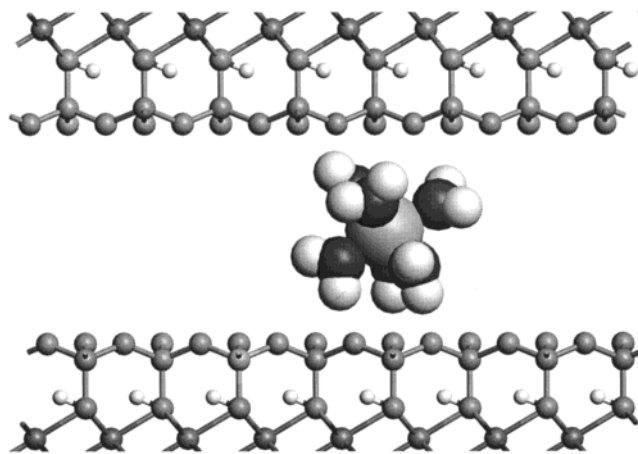


**Figure 1.** Equilibrium MC snapshot of Mg-beidellite in the (*z,x*) plane, showing one Mg<sup>2+</sup> ion (light gray) with its first solvation shell, with remaining interlayer species removed for clarity. Hydrogen atoms in H<sub>2</sub>O or structural OH are white, and water O atoms are shaded dark gray. Starting from the bottom, atoms in the clay mineral are as follows: Al in the octahedral layer, hydroxyl groups and apical O atoms, Si atoms in the tetrahedral layer, and surface O atoms.

configuration from the MC simulations, one in which water molecules had formed solvation shells around the interlayer Mg<sup>2+</sup>, was the initial state. A constant (*N,σ,H*) ensemble, where *σ* = 0, was used instead of the constant (*N,V,U*) ensemble that we have employed in previous MD simulations of hydrated clays.<sup>17,29</sup> In the (*N,σ,H*) ensemble, the layer spacing remains a dynamical quantity and the method of Parrinello and Rahman<sup>33</sup> was used to solve the resulting equations of motion, which replace the usual Newton–Euler equations.<sup>30</sup> The time step was set to 0.25 fs, shorter than the more commonly used 0.5 fs time step<sup>12</sup> to accurately model the strong ion–water interactions. Each simulation began with an equilibration period of 10 ps, in which the desired temperature was maintained with a Nosé–Hoover thermostat.<sup>30,32</sup> Data collection began after an additional 5 ps of simulation without a thermostat. The average mean-square displacement for the water molecules in each system was tabulated and plotted versus simulation time. The self-diffusion coefficient for water, *D<sub>w</sub>*, then was calculated according to the well-known Einstein relation,<sup>29,30</sup>

$$\frac{1}{N} \sum_{i=1}^N \langle |\mathbf{r}_i(t) - \mathbf{r}_i(0)|^2 \rangle = 6D_w t \quad (2)$$

where *r<sub>i</sub>(t)* is the center-of-mass position of a water molecule at time *t*.

### 3. Results

**3.1. Monte Carlo Simulations at 300 K.** After approximately 1 million MC steps, this system reached an equilibrium *d*(001) spacing of 14.29 ± 0.09 Å. Although this average value is slightly smaller than the experimentally observed 14.7 Å spacing,<sup>4</sup> it is close to the 14.4 Å spacing reported for Mg-vermiculite,<sup>4</sup> which also has only tetrahedral charge substitution. Figure 1 shows an equilibrium MC snapshot with all interlayer species removed except for the solvation shell of one Mg<sup>2+</sup> ion. Magnesium ions reside at the midplane (*z* = 7.15 Å), with three solvating molecules positioned above and below. The relative orientation of each solvating water molecule is consistent with the formation of one hydrogen bond to the nearest siloxane surface, reminiscent of the solvation shells of Mg<sup>2+</sup> in Mg-vermiculite.<sup>4</sup> Figure 2 is a MC snapshot of six nonsolvating water molecules adsorbed to the lower siloxane surface in Figure 1. These molecules are tucked into ditrigonal cavities of the

(33) Parrinello, M.; Rahman, A. *J. Appl. Phys.* **1981**, *52*, 7182.

(25) Sposito, G.; Park, S.-H.; Sutton, R. *Clays Clay Miner.* **1999**, *47*, 192–200.

(26) Millot, C.; Soetens, J.-C.; Martins Costa, M. T. C.; Hodges, M. P.; Stone A. J. *J. Phys. Chem. A* **1998**, *102*, 754–770.

(27) Park, S.-H. *MCY vs ASP–W Potential Surface of Water Dimer*; Technical Report, Earth Sciences Division, Lawrence Berkeley National Laboratory, 1999.

(28) Jorgensen, W. L.; Chandrasekhar, J.; Madura, J. D.; Impey, R. W.; Klein, M. L. *J. Chem. Phys.* **1983**, *79*, 926–935.

(29) Chang, F.-R. C.; Skipper, N. T.; Sposito, G. *Langmuir* **1997**, *13*, 2074–2082.

(30) Allen, M. P.; Tildesley, D. J. *Computer Simulations of Liquids*; Clarendon Press: Oxford, 1987.

(31) Skipper, N. T. *MONTE User's Manual*; Department of Physics and Astronomy, University College: London, 1996.

(32) Refson, K. *Comput. Phys. Commun.* **2000**, *126*, 309.

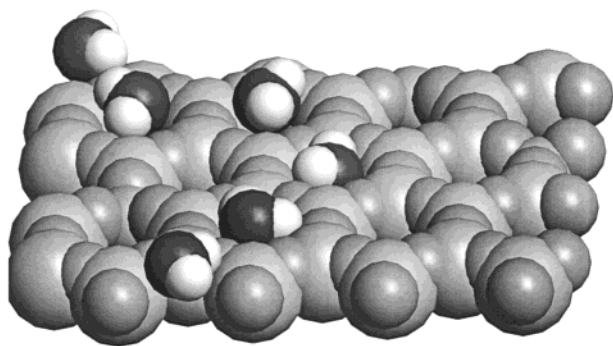


**Figure 2.** Water molecules adsorbed to ditrigonal cavities in the lower siloxane surface. Configuration as in Figure 1.

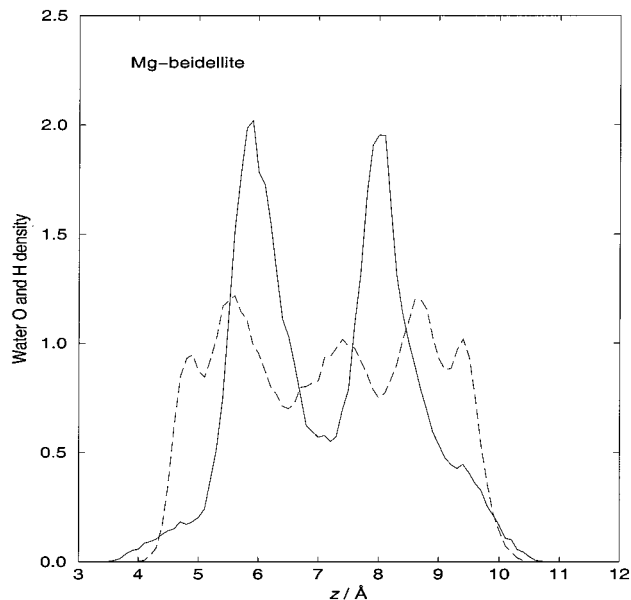


**Figure 3.** Interlayer MC density profiles for water O (solid line) and H (dashed line) atoms in Mg-beidellite. The layer spacing is 14.29 Å, with  $z = 0$  in the center of the octahedral sheet in a clay layer.

siloxane surface and adsorb by forming two hydrogen bonds with the surface. This arrangement of adsorbed water molecules occurs despite the structural hydroxyl being oriented nearly parallel to the basal plane.<sup>18</sup>

Density profiles for the water molecules, averaged over the last one million MC steps, are shown in Figure 3. Water O atoms (solid line) form two broad layers centered at  $z = 5.89$  and  $8.01$  Å, consistent with Figure 1, and the presence of nonsolvating water is evidenced from the long tails in each O profile. The small outer peaks in the water H profile (dashed line) represent both nonsolvating and solvating water molecules. To our knowledge no experimental results have been published on the structure of interlayer water in Mg-beidellite, but X-ray diffraction studies have been performed on Mg-vermiculite with similar water content.<sup>34</sup> Although beidellite, a dioctahedral mineral, differs from vermiculite, a trioctahedral mineral, in quantity and charge of octahedral cations, negative charge sites are located exclusively in the tetrahedral layer of each. The experimental results are summarized by de la Calle and Suquet<sup>34</sup> and references therein, and for the two-layer hydrate of Mg-vermiculite with a  $d(001)$  spacing of 14.3 Å, the fractional  $z$ -coordinates of water molecules were reported at  $z = 0.42$  and  $0.35$  (water in ditrigonal cavities). Using fractional coordinates,

(34) de la Calle, C.; Suquet, H. In *Reviews in Mineralogy*; Bailey, S. W., Ed.; Mineralogical Society of America: Washington, DC, 1988; Vol. 19, pp 476–478.

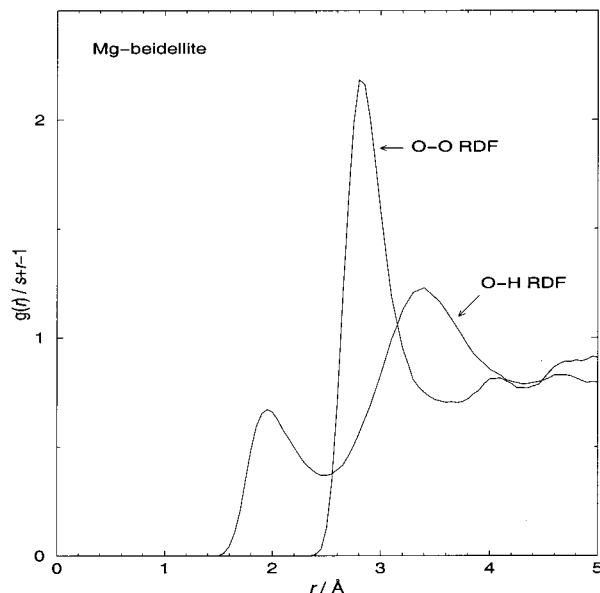


**Figure 4.** Interlayer MC O–O and O–H radial distribution functions (RDFs) for Mg-beidellite. Clay O atoms are included in the RDF calculations.

the first main O peak in Figure 3 occurs at  $z = 0.41$ , and the broad peak due to water in ditrigonal cavities occurs at  $z = 0.34$ . Our results for interlayer water structure are therefore in excellent agreement with experimental results for a similar Mg-substituted clay. Interlayer water structure is depicted in Figure 4 in the form of radial distribution functions, with clay layer O atoms included among the second neighbors in both the O–O and O–H spatial correlations. The peak locations correspond well with those observed by Skipper et al.<sup>13,14</sup> in their MC simulations of Otay-type Mg-montmorillonite, suggesting that  $Mg^{2+}$  solvation is indeed the principal process organizing the interlayer water structure,<sup>16</sup> as opposed to the layer charge distribution.

**3.2. Molecular Dynamics Simulations.** Simulations were performed for Mg-beidellite at 300 (1175 ps) and 400 K (500 ps). Although 500 ps would have been ample simulation time to obtain averaged dynamical data for the 300 K system, the run was extended for the purpose of investigating any two-phase water diffusion behavior. The upper clay layer was restricted to motion in the  $z$ -direction only to prevent registration of negative charge sites in opposing layers. Layer spacings for these two beidellite systems averaged  $14.30 \pm 0.11$  (300 K) and  $14.52 \pm 0.13$  Å (400 K). Cation and water center-of-mass trajectories for the 300 K simulation are shown in Figures 5 and 6. The solvation structure was maintained intact throughout the 300 K simulation (Figure 5). All species within a solvation shell showed limited motion in the  $z$ -direction, but both cation and waters were relatively mobile in the  $x$ - and  $y$ -direction: the  $Mg^{2+}$  ion undergoes a jump along the  $x$ -direction accompanied by water molecules. We also noted that water molecules eventually exchanged in to and out of a solvation shell (data not shown), behavior that has not yet been observed experimentally.<sup>8</sup> Unlike the solvating waters, which moved only about 1 Å in the  $z$ -direction, nonsolvating waters displayed a much greater range of vertical motion. The increased mobility of nonsolvating water molecules, as compared to a water molecule within a solvation shell, is evident in Figure 6, which depicts the trajectories of two such water molecules in the  $(z,x)$  plane. Each occupies interlayer positions on both sides of the midplane and within several of the ditrigonal cavities in the siloxane surface. The nonsolvating water molecules tend to occupy positions within

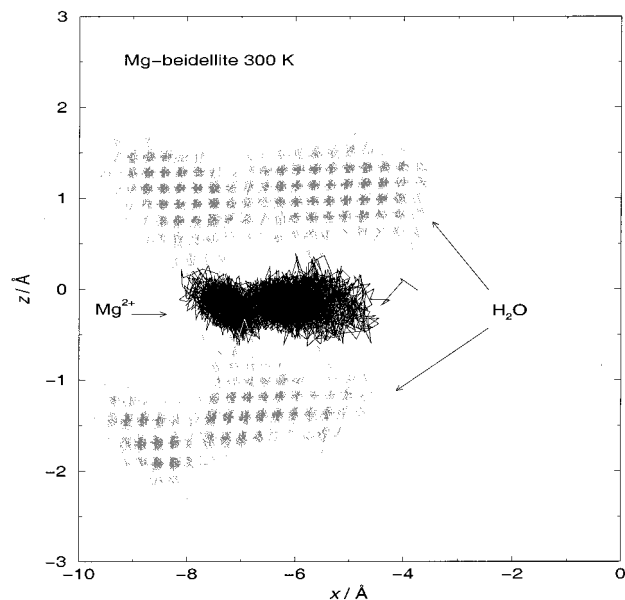


**Figure 5.** Interlayer MD trajectories (over 800 ps) in Mg-beidellite for  $\text{Mg}^{2+}$  (black) and two solvation-shell water molecules (gray), as seen in the  $(z,x)$  plane.

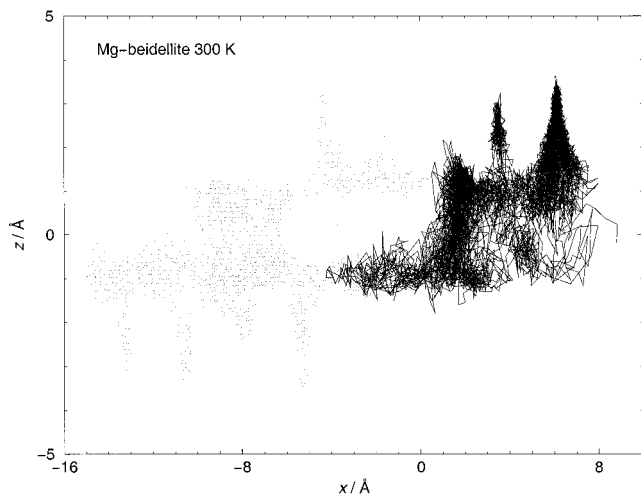


**Figure 6.** Interlayer MD trajectories (over 800 ps) of two nonsolvating water molecules (gray or black), as seen in the  $(z,x)$  plane in Mg-beidellite at 300 K.

a ditrigonal cavity (Figure 2), but the positions of these molecules were not limited to just a single cavity on the MD simulation time scale.

For a comparison with previous MD results on Mg-smectites,<sup>15</sup> a 250-ps MD simulation was also performed at 300 K on an Otay-type Mg-smectite.<sup>13</sup> The Otay-type model consists of a trioctahedral smectite with octahedral layer charge, which is analogous to the hectorite model we have used previously.<sup>17</sup> However, apical O atoms are excluded from the model, in contrast to the beidellite model used in this study. The average layer spacing for the two-layer hydrate of Otay-type Mg-smectite was 14.59 Å (data not shown), in agreement with the experimentally observed and MC-simulated values of 14.7 Å.<sup>4,13,14</sup> Far fewer water molecules are located within the ditrigonal cavities of Otay-type Mg-smectite than for Mg-beidellite, despite the perpendicular orientation of the structural hydroxyl group. An additional factor, which may also affect water adsorption, is the absence of apical O atoms in this early smectite model. However,  $\text{Mg}^{2+}$  maintained an octahedral solvation shell and resided at the interlayer midplane, as in the Mg-beidellite system.

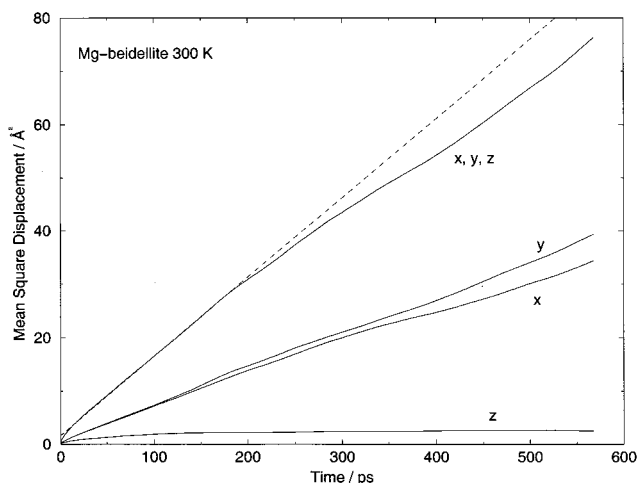


**Figure 7.** Mean-square displacement of water molecules in Mg-beidellite vs time. Solid lines are the  $x$ -,  $y$ -, and  $z$ -components, as well as the sum, whereas the dashed line is the best fit of eq 2 over the time scale 0–175 ps. Note the decreasing rate of water translational motion with time.

**Table 2.** Water Self-Diffusion Coefficients

smectite	$T$ (K)	$D_w$ ( $10^{-10} \text{ m}^2 \text{ s}^{-1}$ )
Mg-beidellite	300	2.48 (0–175 ps)
Mg-beidellite	300	1.99 (175–400 ps)
Mg-beidellite	400	14.4
Bulk liquid	300	23 <sup>a</sup>

<sup>a</sup> Experimental value<sup>9</sup> and MCY bulk-water value.<sup>35</sup>

The  $\text{Mg}^{2+}$  solvation shell and nonsolvating water molecule dynamics were also similar to those of the Mg-beidellite system.

**3.3. Self-Diffusion of Water Molecules.** We show the mean-square displacement (MSD) versus time in Figure 7, and from the individual contributions we see that the  $z$ -component to MSD is negligible. The plot in Figure 7 differs significantly from the form normally expected for diffusional motion, namely a straight line with a small nonzero intercept. From just above zero to 175 ps the MSD is well-fitted by a straight line with a nonzero intercept, just as expected. But at longer times the gradient of the MSD decreases with a fairly abrupt kink at around 175 ps and  $30 \text{ \AA}^2$ . We interpret this shape as evidence that water molecules are able to diffuse relatively freely over distances shorter than  $\sqrt{30} \approx 5.5 \text{ \AA}$  but that diffusion over larger distances is significantly hindered. A length scale of 5.5 Å is characteristic of the periodic repeat of the ditrigonal Si–O rings in the tetrahedral layer and also of the size and separation of the  $\text{Mg}^{2+}(\text{H}_2\text{O})_6$  hydration complexes. Though there is more than one candidate for the mechanism, the evidence for hindered diffusion over longer length-scales is clear. Water self-diffusion coefficients,  $D_w$ , calculated for simulations at 300 and 400 K are given in Table 2. Uncertainties in our calculated values are less than 0.1%. As the last row of Table 2 indicates, the self-diffusion coefficient of pure bulk water calculated using the MCY potential<sup>35</sup> agrees well with experiment.<sup>9</sup>

The most comparable experimental studies of water diffusion in clays are those of Tuck et al.<sup>8</sup> and references therein. Those experiments used quasielastic neutron scattering to probe the rotational and translational diffusional dynamics of water in  $\text{Ca}^{2+}$ - and  $\text{Mg}^{2+}$ -exchanged montmorillonite at the microscopic scale. At a temperature of 300 K, measurements using the low-resolution IN5 instrument, which is sensitive to short-ranged

(35) Madden, P. A.; Impey, R. W. *Ann. N. Y. Acad. Sci.* **1986**, *482*, 91–114.

motion, gave  $D_w = 11.3 \times 10^{-10} \text{ m}^2 \text{ s}^{-1}$  for Ca-montmorillonite, while the high-resolution IN10 instrument, which is sensitive to longer length-scales, yielded a lower result of  $D_w = 3.4 \times 10^{-10} \text{ m}^2 \text{ s}^{-1}$  for both Ca- and Mg-montmorillonite.<sup>8</sup> Furthermore, the scattering angle ( $Q$ ) dependence of the elastic incoherent scattering peak width was interpreted as diagnostic of spatially hindered translational diffusion over a length of 6–7 Å. IN10 measurements were also taken for  $\text{Ca}^{2+}$ - and  $\text{Mg}^{2+}$ -exchanged vermiculite at the same water content (two-layer hydrate), but problems in data analysis led the authors to conclude only that  $D_w \leq 1.0 \times 10^{-10} \text{ m}^2 \text{ s}^{-1}$  for both counterions.<sup>8</sup>

Tuck *et al.*<sup>8</sup> calculated their values of  $D_w$  for the mobile-water fraction only. The other fraction of water molecules, which were attributed to hydration-shell water, showed no evidence of mobility on the time scales accessible to their experiment. Our values of  $D_w$  include solvating water molecules, which account for 18/64, or 28% of the water content, and nonsolvating water molecules, which account for 46/64 (72%) of the water content. Multiplying by a factor of 64/46 results in  $D_w$  values of  $3.45 \times 10^{-10}$  and  $2.77 \times 10^{-10} \text{ m}^2 \text{ s}^{-1}$ , respectively, for the two length-scales at 300 K. Given that the systems—a  $\text{Mg}^{2+}$ -exchanged montmorillonite and vermiculite—differed from our model in layer charge, counterion concentration, and partial pressure of water, these values are not inconsistent with ours. As summarized in Table 2 even the higher value of  $D_w$  is only one tenth of the value in bulk water, showing a substantial hindering of diffusion even at short range by the clay layer and the counterions. Also shown is the higher value obtained from a 400 K simulation showing enhanced diffusion at this temperature.

#### 4. Discussion

Our simulations indicate that the interlayer configuration in the two-layer hydrate of Mg-beidellite is consistent with previous simulations of Mg-smectites,<sup>14,15</sup> with the  $\text{Mg}^{2+}$  situated at the midplane solvated by three water molecules each above and below, in agreement with a number of experimental studies.<sup>4,5,34</sup> Over the time scales of our MD simulations (500–1175 ps), these solvated ions remain in fixed locations near negative charge sites within the clay layers. Nonsolvating water molecules form hydrogen bonds with surface O atoms and move freely on ( $x,y$ ) planes above and below the midplane. However, water

molecules in Mg-beidellite show a greater tendency to occupy ditrigonal cavities in the siloxane surface. The hindered motion of water molecules within such cavities is the likely explanation for the low value of the water self-diffusion coefficient in the Mg-beidellite system (Table 2). These water molecules do not show a preference for cavities with a tetrahedral Al atom on the ditrigonal ring, but the presence of negative charge sites so close to the surface surely results in decreased water mobility. A comparison of water mobility in smectite systems with charge sites in the octahedral layer only (*i.e.*, hectorite) is a topic for future work.

In our MD simulations, only Mg-beidellite at 300 K showed a hindered diffusion process, corresponding to the short- and long-range behavior seen in quasielastic neutron scattering experiments for a similar clay system.<sup>8</sup> According to Figure 7, the transition between these two diffusional phases occurs at a displacement of  $\sqrt{30} \approx 5.5$  Å. A possible cause for the faster diffusional motion on the shorter time scale is that water molecules eventually become trapped in a “cage” of hydrated  $\text{Mg}^{2+}$  ions with length scale  $\approx 6$  Å, although we have noted that this length is also equivalent to the ditrigonal ring dimension in smectites. The fact that such hindered water diffusional behavior has not been seen in MD simulations of clay hydrates with monovalent ions<sup>12,17</sup> suggests that the divalent cation is involved. Tuck *et al.*<sup>8</sup> have suggested that long-range water diffusion is hindered in clay hydrates with a higher layer charge (smectite vs vermiculite). However, in our simulations, a low value of  $D_w$  was observed even though the layer charge in Mg-beidellite is comparatively small: three  $\text{Mg}^{2+}$  for eight unit cells of clay.

**Acknowledgment.** The research reported in this paper was supported in part by the Director, Office of Energy Research, Office of Basic Energy Sciences, of the U.S. Department of Energy under Contract No. DE-AC03-76SF00098. The authors express gratitude to the National Energy Research Scientific Computing Center for allocations of time on its Cray J90 and T3E supercomputers, and to the Oxford Supercomputer Centre for allocations of time on its Silicon Graphics Origin 2000 supercomputer. Thanks to Angela Zabel for excellent preparation of the typescript.

JA0018769